On the performance of existing acoustic energy models when applied to multi-purpose performance halls

Jianliang Gao[a], S.K.Tang[a,*], Yuezhe Zhao[b], Yangsheng Cai[c] and Lili Pan[b]

[a]Department of Building Services Engineering
The Hong Kong Polytechnic University
Hong Kong, China

[b]State Key Laboratory of Subtropical Building Science
South China University of Technology
Guangzhou, China

[c]School of Architecture and Urban Planning
Fujian University of Technology
Fuzhou, China

*Corresponding author,
Email address: shiu-keung.tang@polyu.edu.hk (S.K. Tang)

Abstract

Acoustical measurements were done in two multi-purpose performance halls in the present study. The measured data are compared with predictions from three acoustic energy models in existing literature derived for churches and large reverberant theatres. Results show that the model suitable for the present multi-purpose performance halls is the one which takes into account the time difference between direct sound arrival and onset time of reverberant sound decay. However, unlike the church cases, the time difference appears to have no direct definite relationship with the source-receiver distance alone. A method for the prediction of time difference is then proposed for multi-purpose performance hall application. In addition, the prediction of the late reflected energy is not satisfactory, and this deficiency is the main problem leading to the inaccurate estimation of clarity, definition and centre time in the present study.

1. Introduction

Performance halls are important venues for conducting leisure and cultural activities for the well-being of people. They are essential social facilities especially in congested, busy and highly dynamical cities in which people are stressed by their daily works. They have to cater for many different activities and thus are very often designed for multi-purpose usage. The acoustics inside these performance halls is thus of prime importance and has attracted the attention of many researchers in the past few decades (for instance, Barron [1] and Beranek [2]). There are studies on the subjective evaluations of the hall acoustics [3,4]. There are also investigations focussed on the effects of various indoor architectural features on the acoustical performance of the halls (for instance, Barron [5] and Hidaka et al. [6]).

Apart from the reverberation time (T), the acoustical performance of a performance hall is very often quantified using energy-based acoustical parameters, such as Clarity (C_{80}), Definition (D_{50}), Centre Time (T_s) and Sound Strength (G) [7,8]. These parameters are energy-based and very much related to the impulse response g, from which T is calculated. The prediction of these parameters is therefore an important task in the design stage. The advancement of computational technique and capacity have made the simulation of these parameters possible (for instance, Bork [9]). However, the complex internal geometry of a performance hall and the unknown scattering properties of architectural features and furniture often lead to inaccurate predictions. Therefore, semi-analytical and/or empirical models are applied as they are handier to use without much difference in prediction accuracy in general if auralization is not needed. A good example of the application of sound energy prediction models to acoustic design is presented by D'Orazio et al. [10]. There is recently an effort to relate the interaural cross-correlation coefficients with the geometrical dimensions of a performance hall using empirical/regression formulae [11].

Despite the importance of energy-based acoustical parameters for performance hall design, there are not many semi-analytical models for their predictions to the best knowledge of the authors. The most adopted model for proportionate spaces is that of Barron and Lee [12], which is a revised

version of the classical room acoustics model of Cremer and Müller [13]. There are also prediction models for the church typology, among which those of Cirillo and Martellotta [14-16] and Zamarreño et al. [17] are more extensively studied. Though these models are not usually applied to performance halls, the results of Gao et al. [18] indicate that there are similarities between the acoustical properties of their scaled down opera house model (with a balcony) and the churches. One similarity lies in the significant correlations between energy-based acoustical parameters and source-receiver distance despite some fluctuations, and the other in the over-prediction of overall attenuation of the reflected sound by the theory of Barron and Lee [12]. This suggests that the prediction models developed for the reverberant churches may also be applicable to multi-purpose performance halls. It is therefore worthwhile to examine how these existing acoustic energy models will work for the less reverberant multi-purpose performance halls. This forms one of the major objectives of the present study.

In this study, the monophonic energy-based acoustical parameters C_{80}, D_{50}, T_s and G were measured in two multi-purpose performance halls. We analyse the prediction accuracy of the three abovementioned acoustic energy models when applied to these halls. We also investigate the reasons behind the difference in their performances in order to shed light for further development of prediction model.

2. Acoustic energy models

In the classical room acoustics model, the sound field in a reverberant room is considered to be made up of a direct field and a reverberation field [13]. In the presence of an omni-directional sound source, the sound strength G at a distance r from the source is

$$G(r) = 10\log_{10}\left(\frac{100}{r^2} + \frac{31200T}{V}\right), \tag{1}$$

where V is the volume of the room in concern, T the reverberation time and use has been made of the Sabine's equation. The impulse response function g is

$$g(t) = \frac{13.82 \times 31200}{V} e^{-13.82t/T}, \tag{2}$$

and t = 0 sec represents the instant of direct sound arrival. One can then use Eqs. (1) and (2) to estimate the monophonic energy-based parameters. However, this classical model does not work well for concert halls and large spaces [12]. This leads to various revisions of this theory among which those highlighted in Sec. 1 are more commonly used in practice [10,19,20].

2.1. The revised theory of Barron and Lee [12] (B-L Model)

Barron and Lee [12] observed from their measurements in 17 halls that the total reflected sound level decreases with increasing distance from the source, suggesting that the abovementioned classical theory does not work for large halls with sound absorption on the rear and side walls. They introduced the concept of early and late reflections with an argument that the sound decay at a particular point at a distance r from the source only takes place after the arrival of the direct sound. The impulse response is revised as

$$g_{\mathrm{BL}}(r,t) = \frac{13.82 \times 31200}{V} e^{-0.04r/T} e^{-13.82t/T}. \tag{3}$$

The early reflected energy, E_e, and late reflected energy, E_l, can be obtained by integrating g_{BL} over different time intervals :

$$E_e(r) = \int_0^{\tau} g_{\mathrm{BL}}(r,t)dt \quad \text{and} \quad E_l(r) = \int_{\tau}^{\infty} g_{\mathrm{BL}}(r,t)dt, \tag{4}$$

where the value of τ depends on how one defines "early" and "late". For instance, τ = 80 ms and 50 ms for C_{80} and D_{50} respectively. With the direct sound energy E_d represented by $100/r^2$, one can then obtain the expressions for the energy-based hall parameters adopted in the present study. Details of the formulation can be found in existing literature, such as Zamarreño et al. [17], and thus are not repeated here.

2.2. The "μ-model" for Mudejar-Gothic churches

The measurement results of Sendra et al. [21] in Gothic-Mudejar churches deviate considerably from those predicted by the revised model of Barron and Lee [12]. With the test results obtained in 12 Mudejar-Gothic churches, Zamarreño et al. [17] proposed to replace the factor of 0.04

in Eq. (3) by a constant μ just for the part of the early reflected sound energy (from 0 to 80 ms) in order to improve the prediction accuracy for the church typology. The late reflected sound energy decay follows that proposed by Barron and Lee [12]. The corresponding impulse response is

$$g_{\mu}(r,t)=\begin{cases}\dfrac{13.82\times 31200}{V}e^{-\mu r/T}e^{-13.82t/T} & 0\le t\le\tau\\ \dfrac{13.82\times 31200}{V}e^{-0.04r/T}e^{-13.82t/T} & t>\tau\end{cases}, \tag{5}$$

and τ = 80 ms in Zamarreño et al. [17] In principle, μ is frequency dependent. However, the variation of mid-frequency average μ over the surveyed churches is small such that it is assumed to be 0.13 in Zamarreño et al. [17]

2.3. The model of Cirillo and Martellotta [14-16] (C-M Model)

Cirillo and Martellotta [14] proposed that the exponential decay of reflected sound energy in Romanesque churches started some time after the arrival of direct sound. This time delay, t_R, in the energy decay was found to be proportional to the distance between the receiver and the sound source *r*. They further schematized the early sound energy between the direct sound arrival and the commencement of exponential reflected energy decay to vary linearly with time. The initial energy is assumed to be proportional to the direct sound energy and equals γE_d, where γ can be approximated using the average sound absorption coefficient α and the average sound scattering coefficient, ζ, of the internal surfaces together with the acoustic "mean-free-path" [14,22]. Details of its estimation can be found in existing literature, such as Ref. 14, and thus are not repeated here. The corresponding impulse response is

$$g_{\mathrm{CM}}(r,t)=\begin{cases}\gamma E_d-\left(\gamma E_d-\dfrac{13.82\times 31200}{V}e^{-0.04r/T}e^{-13.82t_R/T}\right)\dfrac{t}{t_R}, & 0\le t\le t_R\\ \dfrac{13.82\times 31200}{V}e^{-0.04r/T}e^{-13.82t/T}, & t>t_R\end{cases}. \tag{6}$$

This scheme was further substantiated by an extensive survey in Italian churches [15].

However, as pointed out by Zamarreño et al. [17], the assumption of a linearly initial decrease of energy density with time makes the mathematical formulation of the model a bit complex. Taking advantage of a more detailed analysis of the fine structure of the early reflections in churches,

Martellotta [16] proposed expressing the reflected energy function in the form of a double-rate decay as a linear combination of two exponential decay functions. This gives a more elegant mathematical formulation and a considerable simplification of the calculations without significant loss in accuracy. According to this refined model, Eq. (6) can be revised as follows:

$$g_{\mathrm{rCM}}(r,t) = A_1 e^{-13.82t/T_1} + A_2 e^{-13.82t/T_2}, \tag{7}$$

where $T_1 = T$ and $A_1(r) = (13.82\times 31200/V)\, e^{-0.04r/T}$, so that the first exponential decay coincides with the theory of Barron and Lee [12], while T_2 and A_2 need to be estimated to fit the modified linear function (Fig. 2 in Ref. 16). As suggested by Martellotta [16], a convenient choice is to assume that $T_2 = 6.91t_R$, so that the center of gravity of the second exponential falls in the middle of the t_R interval, and that $A_2(r) = \gamma E_d - A_1(r)$ so that the initial value of the function g_{rCM} is still γE_d. One needs to determine the time delay t_R, the average sound absorption coefficient α and the average scattering coefficient ζ before this model can be applied.

3. The surveyed halls and measurement procedure

In the present study, measurements were carried out in two unoccupied multi-purpose performance halls with balconies under the proscenium setting. Both halls are of typical contemporary design with upholstered seats, an adjustable proscenium opening, a vertically movable orchestra pit, a huge stage house and an auditorium developed from the classical horseshoe-shaped plan. Elegantly set with balcony and main floor seating accommodating more than 1000 people, the two surveyed halls are predominantly used for cultural activities and performances, such as operas, dramas, musicals, dances, chamber music, mini concerts, variety shows, as well as for hosting conferences and ceremonies. Fig. 1 shows the interior of the two halls. One can note the different type of sound absorption installed on the rear and side walls of the halls. For Hall A, the absorption is of the fabric soft packet type, while those in Hall B are slotted wooden panels with absorbent backing. The basic details of the halls are summarized in Table 1.

Fig. 2 illustrates the floor plans and cross-sections of the surveyed halls. Also presented in Fig. 2 are the locations of the sound source and measurement points adopted in the present study. On each of the floor plans, the dash-dot line denotes the central axis of the hall, while the dashed line indicates where the edge of the balcony parapet is. Measurements have actually been carried out also on the balconies as well as in the upper stalls under the balconies. However, the corresponding data will not be used in this study as Barron and Lee [12] did not consider those data obtained in such areas of halls, while there was no balcony in the churches surveyed by Zamarreño et al. [17] and Cirillo and Martellotta [14,15].

The sound source in the present study was a Brüel & Kjær Type 4296 dodecahedron loudspeaker. It was located at the mid-point of the proscenium setting line with a height of 1.5 m from the stage floor. The measurement points were set 1.2 m above the stall floor, which corresponds to the ear height of a normal seated person. A system consisting of a Brüel & Kjær Type 4189 1/2" microphone and a Brüel & Kjær Type 2690 NEXUS conditional amplifier was adopted as the receiver in the present study.

The software DIRAC [23] was used to provide the maximum-length-sequence signal for the measurement and for recording the mono-aural microphone signals used to generate the impulse responses from which the energy-based acoustical parameters D_{50}, C_{80}, T_s, G and T_{20} in octave bands were calculated. However, the foregoing discussions will be focused on the data in the 500 Hz, 1000 Hz and 2000 Hz octave bands as in Refs. 12, 14 and 17. Throughout the measurements, the octave band impulse-to-noise ratios were kept above 35 dB. Background noise levels in the halls during measurement were around 35 dBA.

Fig. 3 summarizes the octave band reverberation times measured at the locations shown in Fig. 2. Owing to different internal finishing, Hall A was less reverberant than Hall B throughout the whole working frequency range of a performance hall during the measurements. The fabric porous materials in Hall A have resulted in lower reverberation times, especially at high frequencies, and the

wider spatial variations of T_{20}. Also, the T_{20} distributions become less symmetrical in the relatively more absorptive Hall A.

4. Results and discussions

4.1. Various constants of the prediction models

The room volume V is a constant in all of the aforementioned acoustic energy models. For performance halls with large fly towers, such as opera houses, theatres and multi-purpose halls, where the stage house is coupled to the auditorium through the proscenium opening, it is somewhat problematic to assess exactly the acoustic volume "seen" by the sound source. Some authors [20,24,25] proposed that only the volume of the auditorium should be taken into account, excluding the volumes of the stage house, the boxes and the gallery. Garai et al. [19] applied the B-L model [12] to analyze the sound fields in several Italian opera houses and suggested also the use of the auditorium volume alone for calculation when the sound source is on the fore stage or proscenium. Given that the source position adopted in the present study is similar to those of Garai et al. [19], only the auditorium volume is considered in the foregoing analyses.

Apart from auditorium volume, the B-L model [12] requires no special constant and thus is straight-forward for application. In the C-M model [14-16] and the μ-model [17], one needs to estimate the time delay t_R and scattering coefficient ζ, and μ respectively.

The method for estimating t_R in this study follows exactly those of Cirillo and Martellotta [15]. The time delay t_R is the time at which the running sound pressure level decay slope (obtained by linear regression of the running 100 ms length time sequence) first equals the mean decay slope after the start of the decay. Fig. 4 illustrates several examples, two from each surveyed hall in this study, of the sound decay and the location of t_R relative to the start of the decay within the 1000 Hz octave band. The time variations of the correlation coefficients of the linear regressions are also presented. One can notice that the t_Rs so estimated are all more than 80 ms after the instant of minimum correlation coefficient. This is much longer than that recommended by Cirillo and

Martellotta [15]. It is also noticed that t_R does not correlate with T_{20} (not shown here). Unlike the results of Cirillo and Martellotta [15], there is no definite relationship between t_R and the source-receiver distance r within the frequency range from 500 to 2000 Hz (octave band) found in the present study as shown in Fig. 5. The same applies to the measured T_{20} as well (not shown here). The much less reverberant performance halls in this study than the churches of Cirillo and Martellotta [15] is believed to be the main reason for the discrepancy. For the present two halls, the lower reverberance could lead to stronger effects of geometrical parameters other than the source-receiver distance on the variations of acoustical indices. Examples of these parameters are the source azimuthal angle and elevation angle [11] and the architectural shape [26]. Further investigations are needed to determine a reliable t_R estimation method for multi-purpose performance halls.

The estimation of mean scattering coefficient ζ in the present study is much less straight-forward though Cirillo and Martellotta [15] does provide a mean for its estimation using the mean characteristics of the area surrounding the sound source (i.e., the chancel area in churches). However, their scheme is not likely to work in multi-purpose performance halls. In the multi-purpose performance halls, the existence of various absorptions, such as house curtain, soft black masking, fly curtains, cycloramas, backdrops, absorptive panels on stage walls and etc. makes the total sound absorption around the source very dominant [18,27]. The effects of scattering then appear comparatively less prominent. Also, the volume of the stage house is usually very large compared to that of the auditorium. The huge fly tower together with the side stages and back stage in some cases (e.g. Hall B and Gao et al. [18]) results in considerable sound energy radiation into the stage house. The long distance between the source and stage walls will cause relatively weak energy reflection into the auditorium space. Besides, the presence of reflectors and diffusers in performance halls (c.f. Fig. 1) largely influences sound scattering within the auditorium/seating area. All these typological differences between churches and performance halls call for a different sound scattering coefficient estimation scheme for the latter.

In the present study, it is proposed to estimate objectively the mean scattering coefficient ζ using the integrated early reflected energy, i_E [14], in a way similar to that adopted by Zamarreño et al. [17] for determining their constant μ. The integrated early reflected energy is chosen as it has direct and strong relationship with both ζ and t_R [15]. The value of scattering coefficient which results in the lowest RMS deviation from measurements in a hall is taken as the mean scattering coefficient ζ of that particular hall in the present study.

Fig. 6 illustrates how ζs are estimated in the present study. For the less reverberant proscenium Hall A without significant scattering devices around the stage house (Fig. 1a(ii)), ζ appears to decrease with increasing frequency and becomes insignificant at higher frequencies. Sound scattering in Hall B is more significant probably because of its reverberance and the presence of a large diffuser at the stage house (Fig. 1b(ii)). However, there appears no direct relationship between ζs and reverberation times in the two surveyed halls.

The method to estimate μ in this study follows exactly that of Zamarreño et al. [17] using C_{80}. Fig. 7 illustrates the corresponding results. There is no definite trend for the variation of μ with frequency or T_{20}. The present values of μ are significantly less than those of the reverberant churches of Zamarreño et al. [17], but much closer to that proposed by Barron and Lee [12]. The present small μ indicates that the reflected energy (both early and late) is more uniformly distributed in the two surveyed halls than those in Barron and Lee [12] and Zamarreño et al. [17]. Comparing the present results with those of Barron and Lee [12] and Zamarreño et al. [17], it appears that small hall volume tends to reduce μ, and a stronger reverberation in small halls leads to further reduction of μ in general. This is left to further investigation.

4.2. Performance of prediction models

With all the required constants estimated, a comparison between predictions obtained by the abovementioned three common models and site measurements is carried out in a way similar to that of Berardi et al. [28]. The input parameters for the calculations of the monophonic acoustical

parameters are summarized in Table 2. In the present study, the spatially averaged sound absorption coefficients α are calculated from the averaged T_{20} together with the Eyring's formula.

In the foregoing discussions, the energy-based acoustical parameters presented are averaged across the 500 Hz, 1000 Hz and 2000 Hz octave bands. The suffix "mid" hereinafter denotes quantity obtained using this mid-frequency averaging. All the acoustical parameters are calculated at each receiver position using the local T_{20} and the abovementioned prediction models (i.e. the B-L model [12], the μ-model [17] and the refined C-M model [16]). They are then compared with site measurements by means of four indices, namely the mean difference, the mean ratio of just noticeable difference (JND), the prediction accuracy and the slope difference in the first place [15]. The mean JND ratio is estimated as the ratio of the mean absolute difference between predicted and measured values at each receiver position to the JND for the given parameter, which is 1 dB for both G and C_{80}, 5% for D_{50} and 10 ms for T_s [29]. The prediction accuracy is defined as the RMS deviation between predicted and measured values. Linear regressions between the acoustical parameters (both predicted and measured) and the source-receiver distance are performed. The slope difference refers to the difference between the slopes of the respective regression lines.

Table 3 summarizes a comparison between predictions and measurements for the two surveyed halls in an overall average sense. All prediction models give reasonably good estimations for the purely energy-based index G and the refined C-M model [16] gives the best overall prediction. However, for indices which are defined in the form of energy ratio (C_{80}, D_{50} and T_s), the performance of the B-L model [12] and the μ-model [17] are comparable, while that of the refined C-M model [16] is a bit lagging behind, especially for the more reverberant Hall B. It is also noted that the former two models basically give similar overall performance for Hall A, but the μ-model performs slightly better for Hall B. Hall A was less reverberant during the survey and the corresponding mean μ value is near to 0.04 (Table 2), which is the value assumed by Barron and Lee [12] and thus the similar performances of the B-L model and the μ-model for Hall A. The more reverberant Hall B has resulted

in a much smaller mean μ than 0.04, lowering down the performance of the B-L model on predicting the hall averages.

Fig. 8 illustrates the variations of the predicted and measured energy-based acoustical parameters with source-receiver distance. The acoustical parameters are all much less dependent on source-receiver distance than those of the churches and theatres [12,14,15,17]. For the less reverberant Hall A, the measurements and predictions (Fig. 8a) are all close to each other, but those predicted by the refined C-M model [16] appear to scatter over a wider range, except for the case of G_{mid} (Fig. 8a(iv)). One can also notice that the corresponding $C_{80,\text{mid}}$ becomes fairly constant at 6 dB for $r > 10$ m. The early arrival energy is approximately 4 times that of the late arrival one at large distance from the source in Hall A.

For the more reverberant Hall B, the energy-ratio-based acoustical parameters do not vary much with source-receiver distance (Fig. 8b(i) to (iii)). The performances of all the prediction models are unsatisfactory and those of the refined C-M model are the worst. As reverberation has stronger effect on the late energy, it is believed that the unsatisfactory performance of the C-M model could be due to a less accurate prediction of the late arrival energy. However, the refined C-M model predicts very well the sound strength, G_{mid}, showing that this model can give reasonable prediction of the early arrival energy. This will be discussed further later.

One should note that the abovementioned performance indices give an overall view on the general performances of the prediction models. It should be noted the differences could vary substantially from assessment point to assessment point. In order to understand how the models predict local parameters, a point-by-point comparison is done using linear regression analysis and the results are summarized in Table 4. For the less reverberant Hall A, one can see that though the B-L model and μ-model give lower prediction errors for the energy-ratio-based parameters, the predictions do not correlate with the measurements very well and the predictions fall into narrow ranges. On the contrary, the refined C-M model is the best model in term of both absolute prediction

error and spatial variation (slope of regression line ≈ 1) for the prediction of the sound strength G_{mid}, which represents the overall acoustical energy at a particular location in the hall.

All the prediction models fail to predict the spatial variation trends of the acoustical parameters of Hall B, except G_{mid}. The refined C-M model [16] remains the best for the prediction of G for the more reverberant Hall B. The good prediction of G_{mid} for both Hall A and Hall B, but the unsatisfactory predictions of the other acoustical parameters, especially for the more reverberant Hall B, tends to suggest that there is likely to be a deficiency in modelling the early and late arrival energies.

4.3. Early and late arrival energies

As the results associated with $C_{80,\text{mid}}$, $D_{50,\text{mid}}$ and $T_{s,\text{mid}}$ are basically inline with each other, the former is chosen to define "early" and "late" in this section without loss of generality. The early reflected energy, E_{80}, then represents the sum of the reflected acoustical energy arrived at a particular hall location within the first 80 ms after the arrival of the direct sound (energy E_d). The late reflected energy E_l denotes the sum of all the energy arrived afterward. Therefore, the mid-frequency sound strengths are

$$G_{\text{mid}} = 10\log_{10}\left(E_d + E_{80,\text{mid}} + E_{l,\text{mid}}\right),$$

$$G_{80,\text{mid}} = 10\log_{10}\left(E_d + E_{80,\text{mid}}\right) \text{ and } G_{l,\text{mid}} = 10\log_{10}\left(E_{l,\text{mid}}\right) \tag{8}$$

after the usual energy normalization (for instance, Barron and Lee [12]). The clarity is thus basically

$$C_{80,\text{mid}} = 10\log_{10}\left(\frac{E_d + E_{80,\text{mid}}}{E_{l,\text{mid}}}\right) = G_{80,\text{mid}} - G_{l,\text{mid}}. \tag{9}$$

Table 5 illustrates the average discrepancies between predictions and measurements of the early and late energies. For Hall A, the three models in general give similar overall performance. However, the refined C-M model gives significantly better prediction of $G_{80,\text{mid}}$ for the more reverberant Hall B. For both surveyed halls, the overall prediction of $G_{l,\text{mid}}$ is not satisfactory, especially for Hall B.

Fig. 9 summarizes the variations of both measured and predicted $G_{80,mid}$ and $G_{l,mid}$ with the source-receiver distance r. For Hall A, which is much less reverberant than the churches and theatres of Barron and Lee [12], Cirillo and Martellotta [14,15] and Zamarreño et al. [17], the late arrival energies in Hall A are weak compared to the early arrival ones, such that $G_{mid} \sim G_{80,mid}$ (Figs. 8a(iv) and 9a(i)). As discussed earlier, the refined C-M model [16] predicts well the spatial variation of these sound strengths. The other two models assume exponential decay of sound energy right after the arrival of direct sound, resulting in overestimation of the early energy especially when the large space in concern is absorptive. The multi-purpose performance halls in the present study fall into such category. The larger the distance from the source, the worse will be the overestimation. The refined C-M model [16] slightly underestimates $G_{80,mid}$ for $r > 14$ m (Fig. 9a(i)), probably because of the reflection from the balcony, which tends to strengthen the early sound. Such phenomenon is not included in the three prediction models.

The prediction of $G_{l,mid}$ for Hall A is not successful as shown in Fig. 9a(ii). While the B-L model and the μ-model tend to overestimate $G_{l,mid}$ in general, the refined C-M model could result in large underestimation. Since the C-M model gives good prediction of or slightly underestimates the early energy but occasionally large underestimations of the late energy, the corresponding $C_{80,mid}$s deviate more from the measurement than those predicted by the other two models on average. This applies also to $D_{50,mid}$ and $T_{s,mid}$.

The other two models give better overall prediction errors of $C_{80,mid}$ and $D_{50,mid}$ not because they are better models. They just overestimate both the early and late energies in similar proportions. This further illustrates that these two models may not be so applicable to multi-purpose performance halls as they overestimate very much the late energies, such that a lower μ than 0.04 is required in the μ-model to overestimate the early energies in order to reduce the prediction errors of energy ratios. It should be noted that a small μ has an effect similar to reducing source-receiver distance, there will therefore be a risk of overestimating G_{80} in general.

For the more reverberant Hall B (though it is still not as reverberant as those surveyed by the others [12,18]), the magnitude of the late energy is closer to that of the early energy and thus G_{mid} is obviously greater than $G_{80,\mathrm{mid}}$ (Figs. 8b(iv) and 9b(i)). For Hall B, the refined C-M model gives good prediction of $G_{80,\mathrm{mid}}$, while the other two overestimates the parameter. All the three models result in very similar overestimations of $G_{l,\mathrm{mid}}$ (Fig. 9b(ii)), though the refined C-M model gives slightly better match. The overestimation increases with increasing source-receiver distance in general. One can also notice from Figs. 9a(ii) and 9b(ii) that there is a decay of ~3 dB of $G_{l,\mathrm{mid}}$ when r is increased from 10 m to 20 m.

Table 6 illustrates the correlations between the predicted and measured sound strengths. Similar to those presented in Table 4, the refined C-M model [16] gives the best correlations for G_{mid} and $G_{80,\mathrm{mid}}$. The slopes of the corresponding regression lines are again close to unity, suggesting that the predicted sound strengths differ from the measurement by roughly some constants in general. The approach adopted in this model can be the best among those of the three tested models should the prediction of the late reflected energy be improved and a method to estimate t_R be established. More multi-purpose performance hall surveys are required before a better picture can be sought.

4.4. A revised estimation of t_R

In order to avoid the significantly scattered prediction results of the refined C-M model and to allow a possible practical use of the present results, a new method for the estimation of t_R is proposed to replace the point-by-point determination adopted in earlier sections. Cirillo and Martellotta [14] found that t_R was proportional to the source-receiver distance r and expressed this relationship as $t_R = \rho r$. An intermediate quantity, $t_{R\max}$, was introduced to calculate the proportionality coefficient ρ (Eq. (13) in Ref. 14). $t_{R\max}$ was defined as the time delay necessary to achieve a sufficiently high reflection density (N), and

$$t_{R\max} = \sqrt{\frac{VN}{4\pi c^3}}, \tag{10}$$

where c is the sound speed in air. Given that t_R in a hall cannot exceed $t_{R\max}$ and that there is no

significant relationship between t_R and r observed in the present study (Fig. 5), it is proposed to take $t_{R\max}$ as the value of t_R. However, the temporal density of sound reflections arriving at that time, N, has to be determined in order to estimate t_R.

It is reasonable to assume that a more reverberant sound field should have a higher temporal reflection density. Therefore, N should increase with the reverberation time. In order to quantify the relationship between N and reverberation time, a regression analysis is conducted using the octave band data between 500 Hz to 2000 Hz collected in the two surveyed halls in the present study. In this analysis, the octave band values of N are obtained using Eq. (10), with $t_{R\max}$s (thus t_R) estimated through minimizing the overall deviation of the predicted G_{80} in a way similar to the determination of scattering coefficient (Fig. 6) and μ coefficient (Fig. 7) as shown in Fig. 10. The corresponding result is shown in Fig. 11.

As $N = 0$ reflection/s under anechoic condition ($T = 0$ s), the best linear line that fits the present hall data and passes through the origin is determined and given in Fig. 11. In addition, the church data of Cirillo and Martellotta [14] are used as a reference for comparison. It is found that the current regression line coincides with the result of Cirillo and Martellotta [14] though the present halls are much less reverberant than their churches. It appears that the existence of a linear relationship between N and reverberation time is very likely. It is left to further investigations. The regression line obtained after including the data of Cirillo and Martellotta [14] is $N = 230T_{20}$. Therefore, the formula for t_R is proposed as

$$t_R = \sqrt{\frac{230TV}{4\pi c^3}}\,. \tag{11}$$

The t_Rs estimated using Eq. (11), the measured average reverberation times and Ns are listed in Table 7. It can be found together with the data presented in Fig. 10 that the newly estimated t_Rs using Eq. (11) give predictions very close to those for the minimum G_{80} deviations. The hall average t_Rs and T_{20}s given in Table 7 are used in the foregoing analysis, unless otherwise specified. As the average reverberation time can be calculated using the hall volume V and the overall hall acoustic

absorption A by means of the Sabine's formula ($T = 0.161V/A$), the t_R values can thus be predicted even without any physical measurement (for instance, during the design stage of a hall).

Figure 12 shows the variation of RMS deviations before and after using the newly proposed t_R estimation. It is observed that the application of the newly estimated t_Rs to the refined C-M model can further improve the prediction accuracy of $G_{80,\mathrm{mid}}$ for the two surveyed halls in the present study (Fig. 12a). For $G_{l,\mathrm{mid}}$ and G_{mid}, there is a slight improvement in the predictions related to the less reverberant Hall A. However, there is a slight increase in the prediction errors of $C_{80,\mathrm{mid}}$, $D_{50,\mathrm{mid}}$ and $T_{s,\mathrm{mid}}$ (Figs. 12d to 12f). In general, the prediction errors resulting from the proposed t_R estimation are quite similar to those discussed earlier for all the energy-based acoustical parameters so that the relative performance between the three energy models presented earlier remains unchanged basically. Figures 13 and 14 give a point-by-point comparison between measurements and the energy-based parameters predicted by the refined C-M model using point-by-point t_Rs as well as hall averaged t_Rs. As expected, adopting hall averaged t_R in each octave band (Table 7) instead of those estimated point by point (Fig. 5) does lead to less scattered prediction results.

5. Conclusions

Measurements of monophonic energy-based acoustical parameters were carried out in two multi-purpose performance halls in the present study. The performances of three existing energy-based models, including those from Barron and Lee [12], Zamarreño et al. [17] and Martellotta [16], on estimating these acoustical parameters, were examined. It should be noted that the multi-purpose performance halls are designed to be used for both musical, concerts and speeches. Thus, they are much less reverberant than those churches and theatres surveyed by the abovementioned researchers.

The results show that all the adopted prediction models do not predict satisfactorily the late sound strength. The model of Martellotta [16], which includes a time difference between the direct sound arrival and the instant of exponential sound decay (on-set of reverberation), gives reasonable prediction of the early sound strength and its spatial variation. It is probably because of the more

absorptive halls in the present study. However, the time differences recorded in the present multi-purpose performance halls do not show any dependence on source-receiver distance, so a new estimation method is proposed in this study. This method not only results in less scattered values of predicted parameters, but also enables a possible practical use of the present results, which are obtained based on the model of Martellotta [16]. The other two models overestimate the early sound strengths.

Owing to the overestimations of both the early and late sound strengths by the models of Barron and Lee [12] and Zamarreño et al. [17], these two models tend to give clarities, definitions and centre times closer to the measurements than that of Martellotta [16]. They are not more accurate models by themselves. It is clearly evidenced that the main challenge to improve the prediction accuracy for the multi-purpose performance hall typology is on the modelling of the late sound strength or the late reflected energy. The prediction of the time difference between direct sound arrival and the on-set of reverberation in multi-purpose performance halls, which are usually much less reverberant than churches, also worth further investigations.

Acknowledgments

Jianliang Gao was supported by a studentship from the Research Committee, the Hong Kong Polytechnic University. Yangsheng Cai was supported by the New Century Excellent Talent Program of the Fujian Province University. The authors would also like to thank Prof Shuoxian Wu of the South China University of Technology for his continuous interest in and support on the present work.

References

[1] Barron M. Auditorium Acoustics and Architectural Design. 2nd ed. Oxon: Spon; 2010.

[2] Beranek LL. Concert Halls and Opera Houses. 2nd ed. New York: Springer; 2004.

[3] Farina A. Acoustic quality of threates: correlations between experimental measures and subjective evaluations. Appl Acoust 2001; 62(8): 889 – 916.

[4] Lokki T, Pätynen J, Kuusinen A, Vertanen H, Tervo S. Concert hall assessment with individually elicited attributes. J Acoust Soc Am 2011; 130(2): 835 – 849.

[5] Barron M. Balcony overhangs in concert auditorium. J Acoust Soc Am 1995; 98(5): 2580 – 2589.

[6] Hidaka T, Beranek LL, Masuda M, Nishihara N, Okano T. Acoustical design of Tokyo Opera City (TOC) concert hall, Japan. J Acoust Soc Am 2000; 107(1): 340 – 354.

[7] Kutturff H. Room acoustics. Oxon: Spon; 2009.

[8] Cheung LY, Tang SK. Neural network predictions of acoustical parameters in multi-purpose performance halls. J Acoust Soc Am 2013; 134(3): 2049 – 2065.

[9] Bork I. A comparison of room simulation software – the 2nd Round Robin on room acoustical computer simulation. Acta Acust u Acust 2000; 86(6): 943 – 956.

[10] D'Orazio D, Fratoni G, Garai M. Acoustics of a chamber music hall inside a former church by means of sound energy distribution. Can Acoust 2017; 45(4): 7-17.

[11] Cheung LY, Tang SK. Geometrical parameter combinations that correlate with early interaural cross-correlation coefficients in a performance hall. J Acoust Soc Am 2016; 139(5): 2741 – 2753.

[12] Barron M, Lee LJ. Energy relations in concert auditoriums. I. J Acoust Soc Am 1988; 84(2): 618 – 628.

[13] Cremer L, Müller HA. Principles and Applications of Room Acoustics, Vol. 1. London: Applied Science; 1982.

[14] Cirillo E, Martellotta F. An improved model to predict energy-based acoustic parameters in Apulian-Romanesque churches. Appl Acoust 2003; 64(1): 1 – 23.

[15] Cirillo E, Martellotta F. Sound propagation and energy relations in churches. J Acoust Soc Am 2005; 118(1): 232 – 248.

[16] Martellotta F. A multi-rate decay model to predict energy-based acoustic parameters in churches. J Acoust Soc Am 2009; 125(3): 1281 – 1284.

[17] Zamarreño T, Girón S, Galindo M. Acoustic energy relations in Mudejar-Gothic churches. J Acoust Soc Am 2007; 121(1): 234 – 250.

[18] Gao J, Tang SK, Zhao Y, Wu S. Applicability analysis of the revised acoustic energy model for concert auditoriums to predict energy relations in a scaled opera house. Proc. INTERNOISE 2017. Hong Kong: China; 2017.

[19] Garai M, De Cesaris S, Morandi F, D'Orazio D. Sound energy distribution in Italian opera houses. POMA 2016; 28: Paper No. 015019.

[20] Prodi N, Pompoli R, Martellotta F, Sato S. Acoustics of Italian historical opera houses. J Acoust Soc Am 2015; 138(2): 769 – 781.

[21] Sendra JJ, Zamarreño T, Navarro J. An analytical model for evaluating the sound field in Gothic-Mudejar churches. In: Kenny J, Ciskowski RD, Brebbia CA, editors. Computational Acoustics and its Environmental Applications II. Southampton: Computational Mechanics; 1997, p. 139 – 148.

[22] Vorländer M. Revised relation between the sound power and the average sound pressure level in rooms and consequences for acoustic measurements. Acustica 1995; 81(4): 332 – 343.

[23] DIRAC 4.1, Dual Input Room Acoustics Calculator. Denmark: Acoustics Engineering; 2008.

[24] Hidaka T, Beranek LL. Objective and subjective evaluations of twenty-three opera houses in Europe, Japan, and the Americas. J Acoust Soc Am 2000; 107(1): 368 – 383.

[25] Stanzial D, Bonsi D, Prodi N. Measurement of new energetic parameters for the objective characterization of an opera house. J Sound Vib 2000; 232(1): 193–211.

[26] Jurkiewicz Y, Wulfrank T, Kahle E. Architectural shape and early acoustic efficiency in concert halls. J Acoust Soc Am 2012; 132(3): 1253 – 1256.

[27] Jeon JY, Kim JH, Ryu JK. The effects of stage absorption on reverberation times in opera house seating areas. J Acoust Soc Am 2015; 137(3): 1099 – 1107.

[28] Berardi U, Cirillo E, Martellotta F. A comparative analysis of acoustic energy models for churches. J Acoust Soc Am 2009; 126(4): 1838 – 1849.

[29] ISO 3382-1. Acoustics – Measurement of room acoustic parameters – Part 1: Performance spaces. Geneva: ISO; 2009.

Captions

Figure 1 Interiors of the surveyed halls.

Figure 2 Dimensions of the surveyed halls and measurement points

□ : Sound source; ○ : measurement point; – – – – : balcony edge location;

— · — : hall central axis.

Figure 3 Reverberation time distributions in the stall areas of the halls not under balconies.

Boxes indicate the $5^{th}/95^{th}$, $10^{th}/90^{th}$, $25^{th}/75^{th}$ percentiles and the median;

····· : mean value.

White boxes : Hall A; grey boxes : Hall B.

Figure 4 Estimation of t_R within 1000 Hz octave band as an example.

(a) Hall A; (b) Hall B;

(i) Sound level decay;

(ii) difference between the 100 ms running decay slope and the mean decay slope;

(iii) time variations of correlation coefficients of the linear regression.

——— : Case of longest T_{20}; – – – – : case of shortest T_{20};

○ : instant of running decay slope first equals mean decay slope.

Figure 5 Variations of t_R with source-receiver distance r in the octave bands from 500 Hz to 2000 Hz.

(a) Hall A; (b) Hall B.

○ : 500 Hz; □ : 1000 Hz; △ : 2000 Hz.

Figure 6 Estimation of the mean scattering coefficient ζ.

(a) Hall A; (b) Hall B.

——— : 500 Hz; – – – – : 1000 Hz; — · — : 2000 Hz.

Figure 7 Estimation of hall averaged μ.

(a) Hall A; (b) Hall B.

——— : 500 Hz; – – – – : 1000 Hz; — · — : 2000 Hz.

Figure 8 Variations of predicted and measured acoustical parameters with source-receiver distance.

(a) Hall A; (b) Hall B;

(i) $C_{80,mid}$; (ii) $D_{50,mid}$; (iii) $T_{s,mid}$; (iv) G_{mid};

● : measurement; ○ : Barron and Lee [12]; □ : μ-model [17]; △ : Martellotta [16].

Figure 9 Predictions of early and late sound strengths.

(a) Hall A; (b) Hall B.

(i) $G_{80,mid}$; (ii) $G_{l,mid}$.

● : measurement; ○ : Barron and Lee [12]; □ : μ model [17]; △ : Martellotta [16].

Figure 10 Estimation of hall averaged t_R for minimum G_{80} deviation.

(a) Hall A; (b) Hall B.

——— : 500 Hz; – – – – : 1000 Hz; — · — : 2000 Hz.

Figure 11 Correlation between N and hall averaged T_{20}.

● : Hall A; ■ : Hall B; ▲: Church data [14];

——— : regression line obtained without the church data;

– – – – : regression line obtained with the church data.

Figure 12 RMS deviations between measured and predicted energy-based acoustical parameters obtained using different t_R estimation methods.

(a) $G_{80,mid}$; (b) $G_{l,mid}$; (c) G_{mid}; (d) $C_{80,mid}$; (e) $D_{50,mid}$; (f) $T_{s,mid}$.

Black bar : point-by-point estimated t_R; grey bar : t_R by Eq. (11).

Figure 13 Comparison between predictions of the refined C-M model for sound strengths using the point-by-point estimated t_Rs and the hall averaged t_Rs.

(a) Hall A; (b) Hall B.

(i) $G_{80,mid}$; (ii) $G_{l,mid}$; (iii) G_{mid}.

● : measurements; × : point-by-point estimated t_R ;

○ : hall averaged t_R (Eq. (11)) and local T_{20};

——— : hall averaged t_R (Eq. (11)) and hall averaged T_{20}s.

Figure 14 Comparison between predictions of the refined C-M model for clarity, definition and centre time using the point-by-point estimated t_Rs and the hall averaged t_Rs.

(a) Hall A; (b) Hall B.

(i) $C_{80,\mathrm{mid}}$; (ii) $D_{50,\mathrm{mid}}$; (iii) $T_{s,\mathrm{mid}}$.

Legends : same as those of Fig. 13.

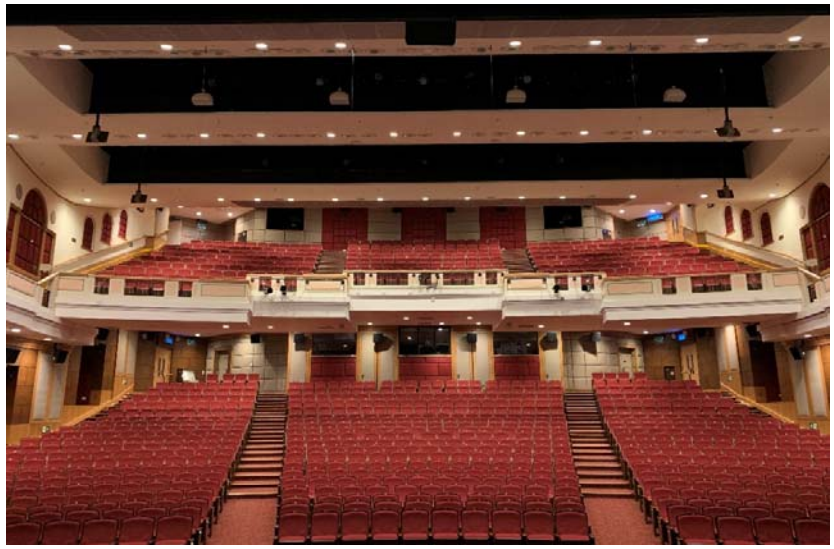

(i) Audience side

(ii) Stage

(a) Hall A

(i) Audience side

(ii) Stage

(b) Hall B

Fig. 1 Interiors of the surveyed halls.

Figure 2

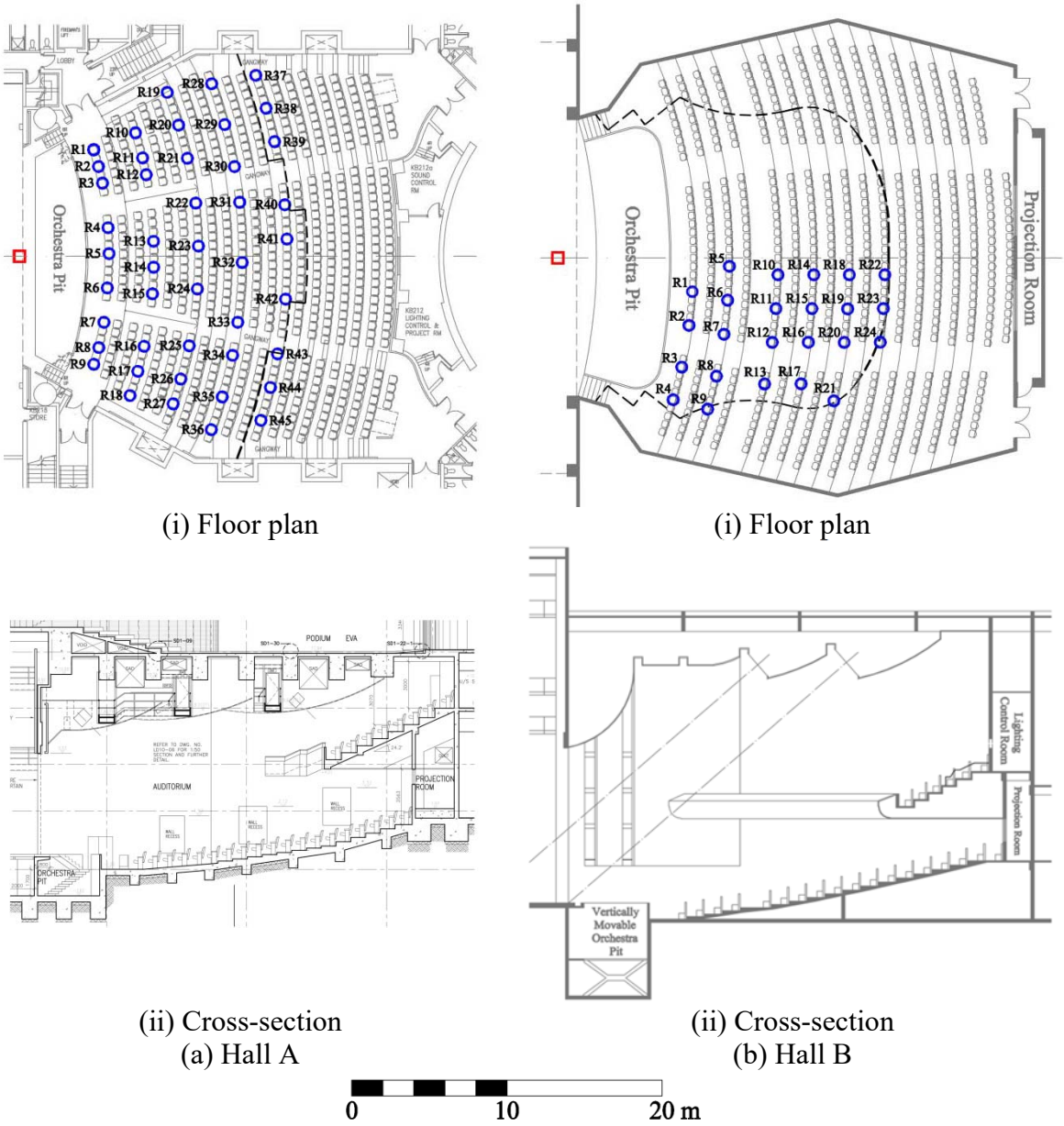

(i) Floor plan

(i) Floor plan

(ii) Cross-section
(a) Hall A

(ii) Cross-section
(b) Hall B

Fig. 2 Dimensions of the surveyed halls and measurement points
□ : Sound source; ○ : measurement point; – – – – : balcony edge location;
— · — : hall central axis.

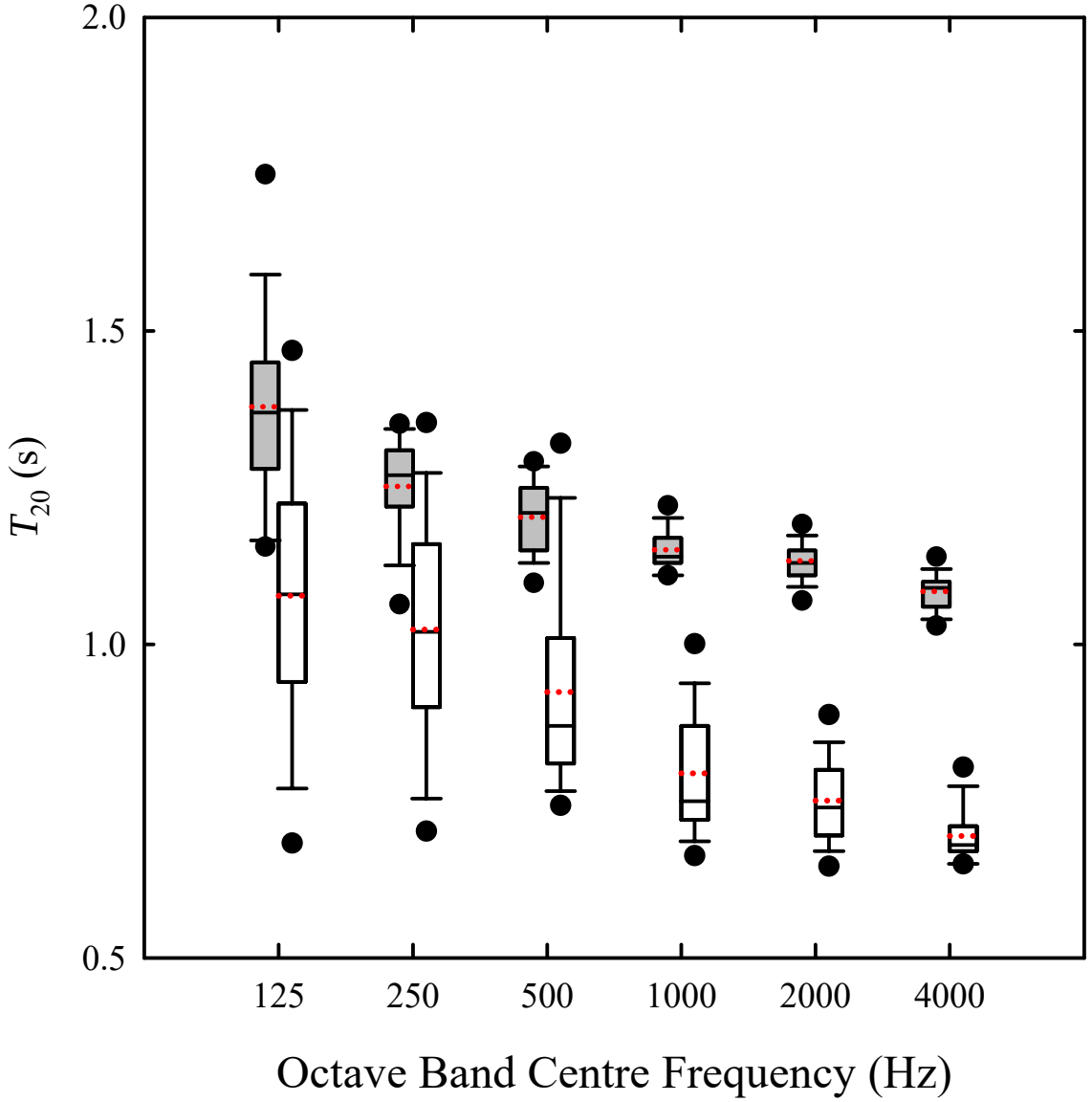

Fig. 3 Reverberation time distributions in the stall areas of the halls not under balconies
Boxes indicate the $5^{th}/95^{th}$, $10^{th}/90^{th}$, $25^{th}/75^{th}$ percentiles and the medium;
····· : mean value.
White boxes : Hall A; grey boxes : Hall B.

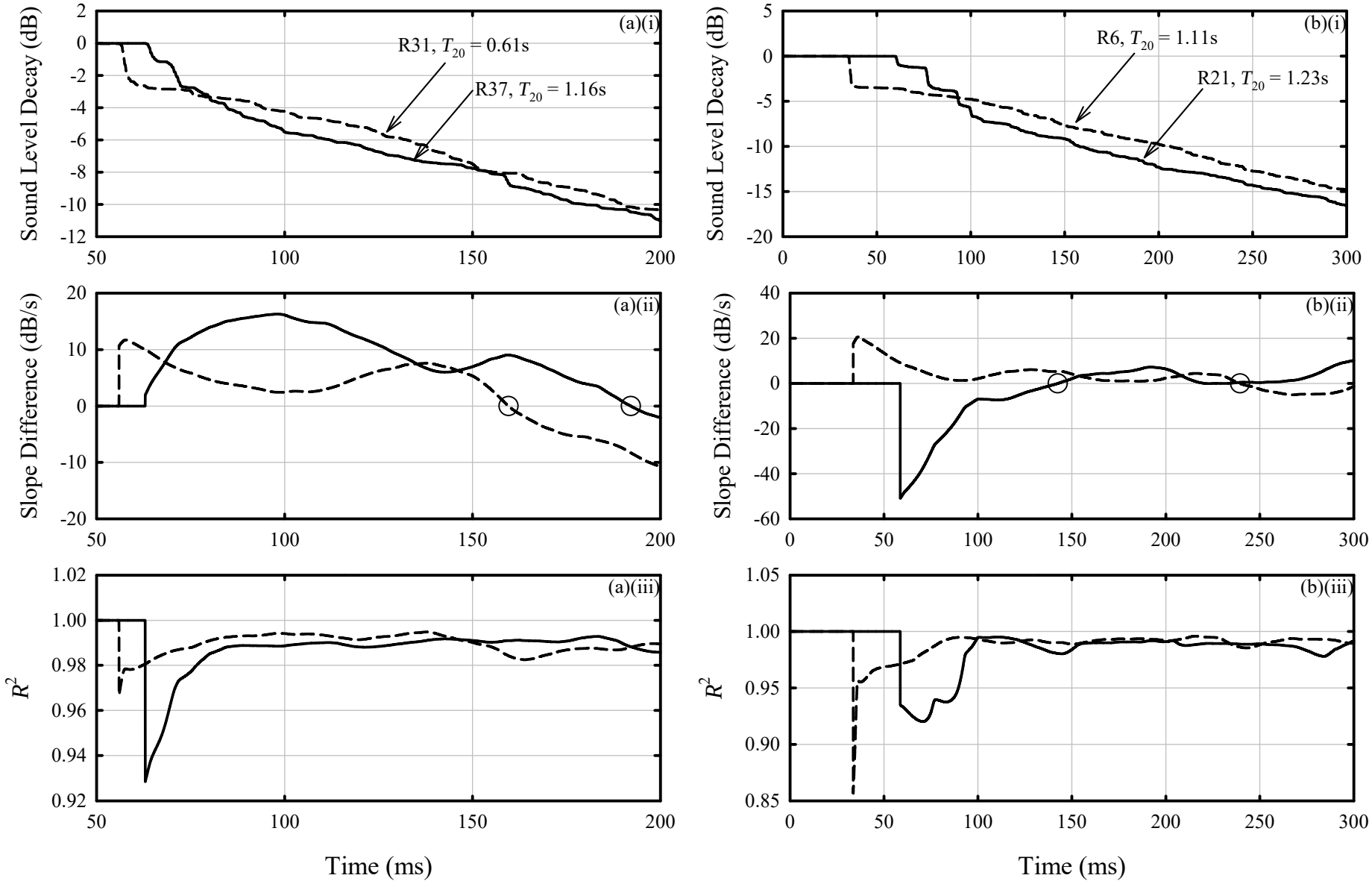

Fig. 4 Estimation of t_R within 1000 Hz octave band as an example.
(a) Hall A; (b) Hall B;
(i) Sound level decay; (ii) difference between 100 ms running decay slope and mean decay slope;
(iii) time variations of correlation coefficients of the linear regression.
—— : Case of longest T_{20}; – – – : case of shortest T_{20}; ○ : instant of running decay slope first equals mean decay slope.

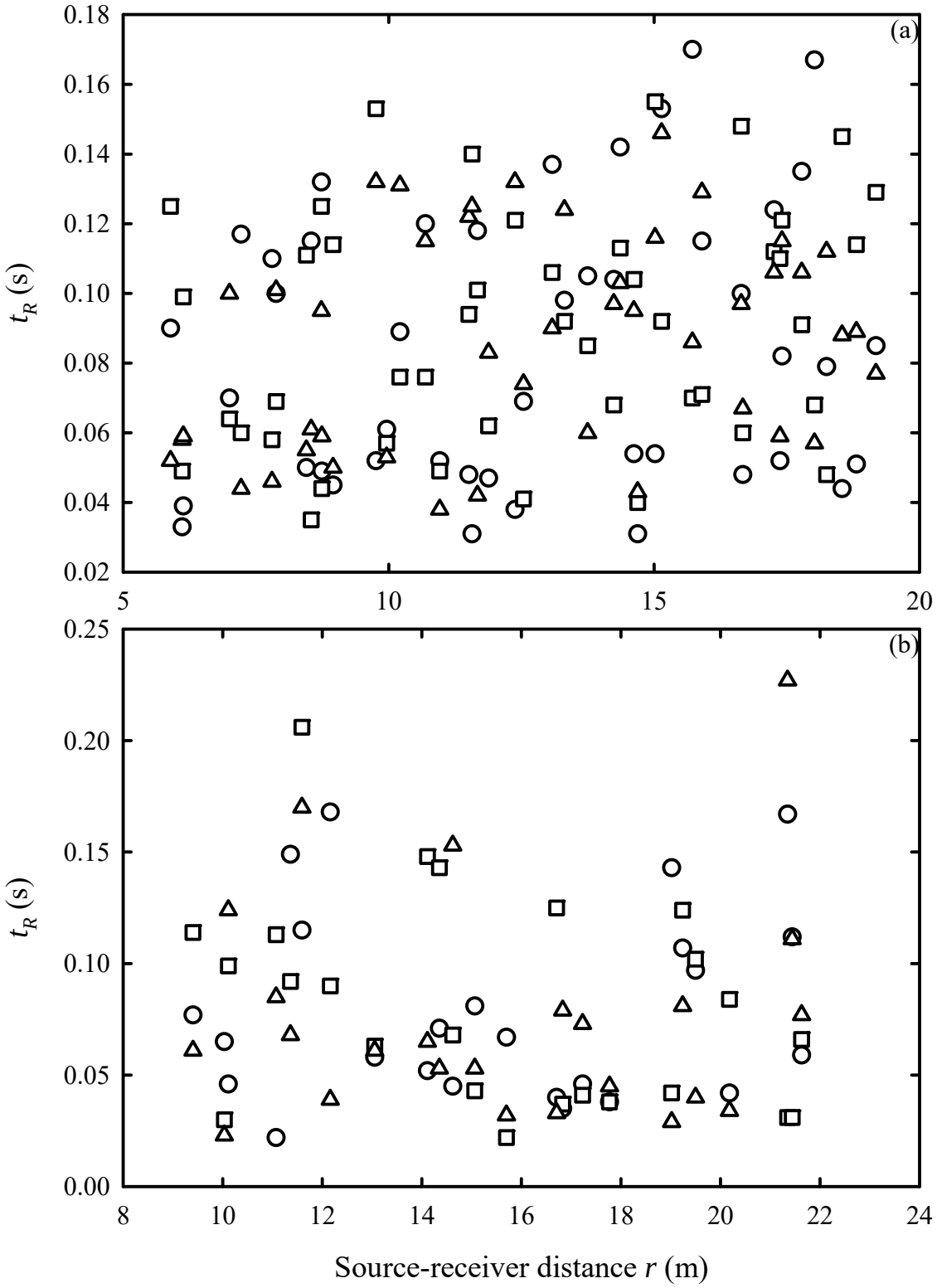

Fig. 5 Variations of t_R with source-receiver distance r in the major aural octave bands.
(a) Hall A; (b) Hall B.
○ : 500 Hz; □ : 1000 Hz; △ : 2000 Hz.

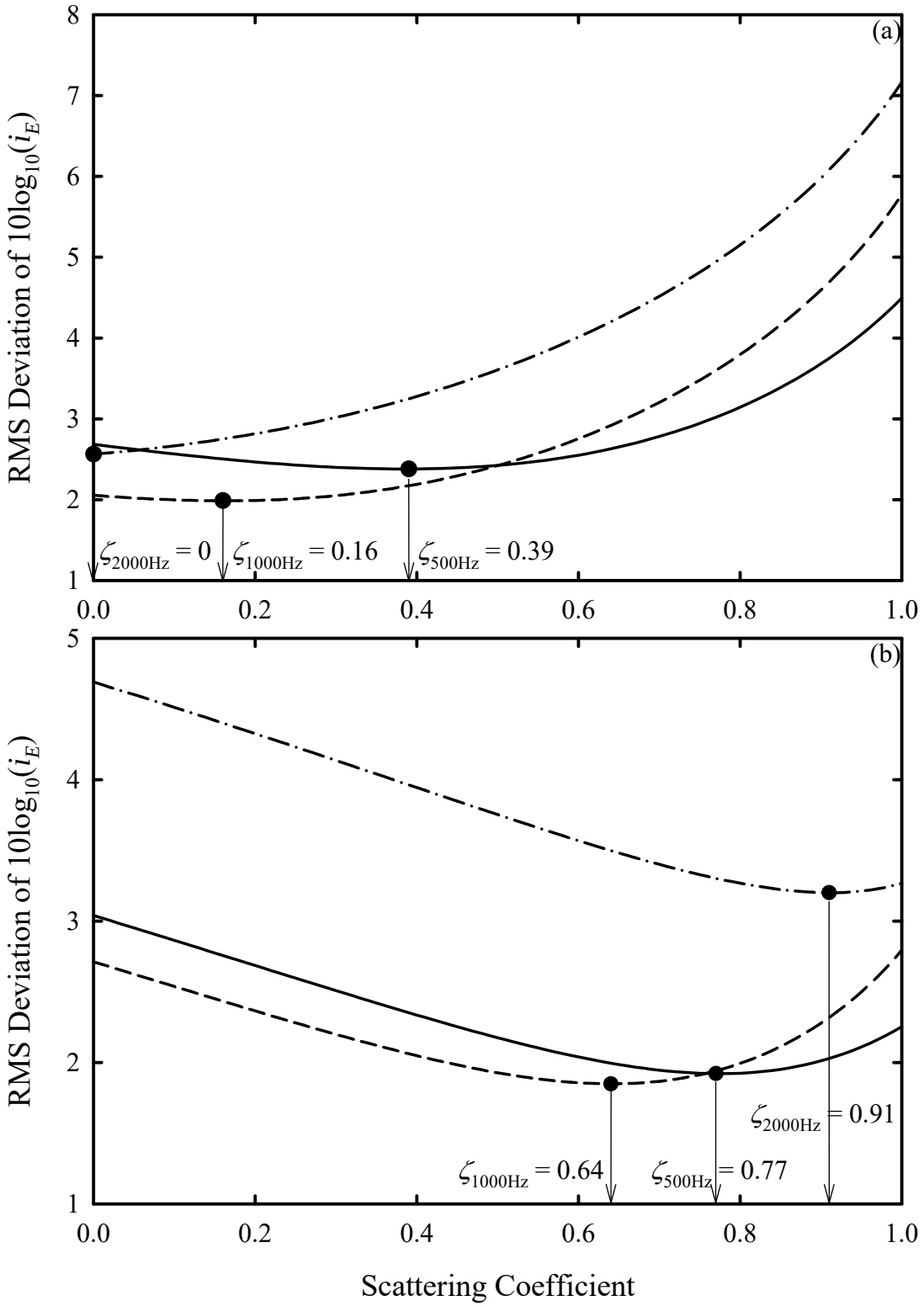

Fig. 6 Estimation of the mean scattering coefficient ζ.
(a) Hall A; (b) Hall B.
——— : 500 Hz; – – – – : 1000 Hz; — · — : 2000 Hz.

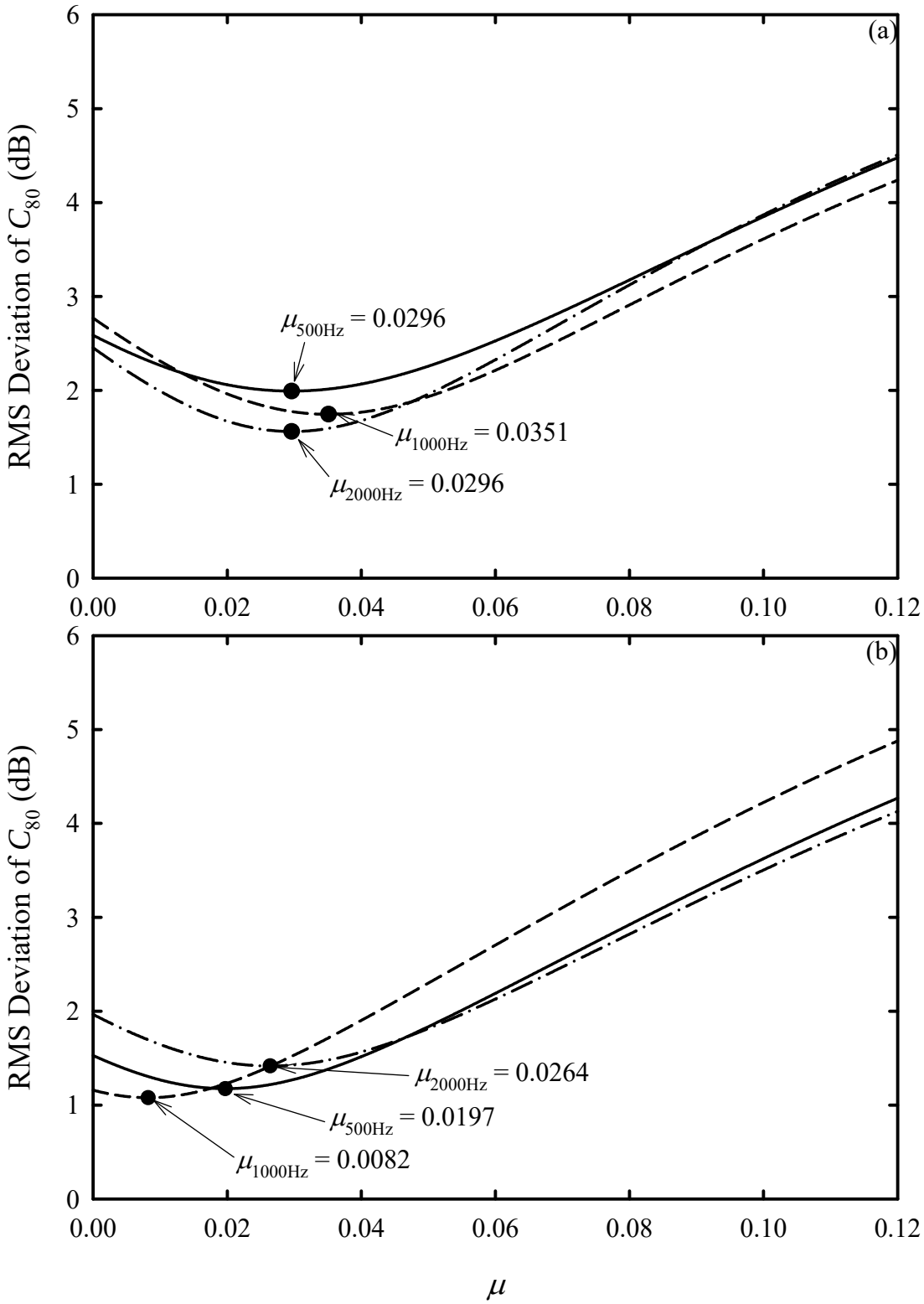

Fig. 7 Estimation of hall averaged μ.
(a) Hall A; (b) Hall B.
——— : 500 Hz; – – – – : 1000 Hz; — · — : 2000 Hz.

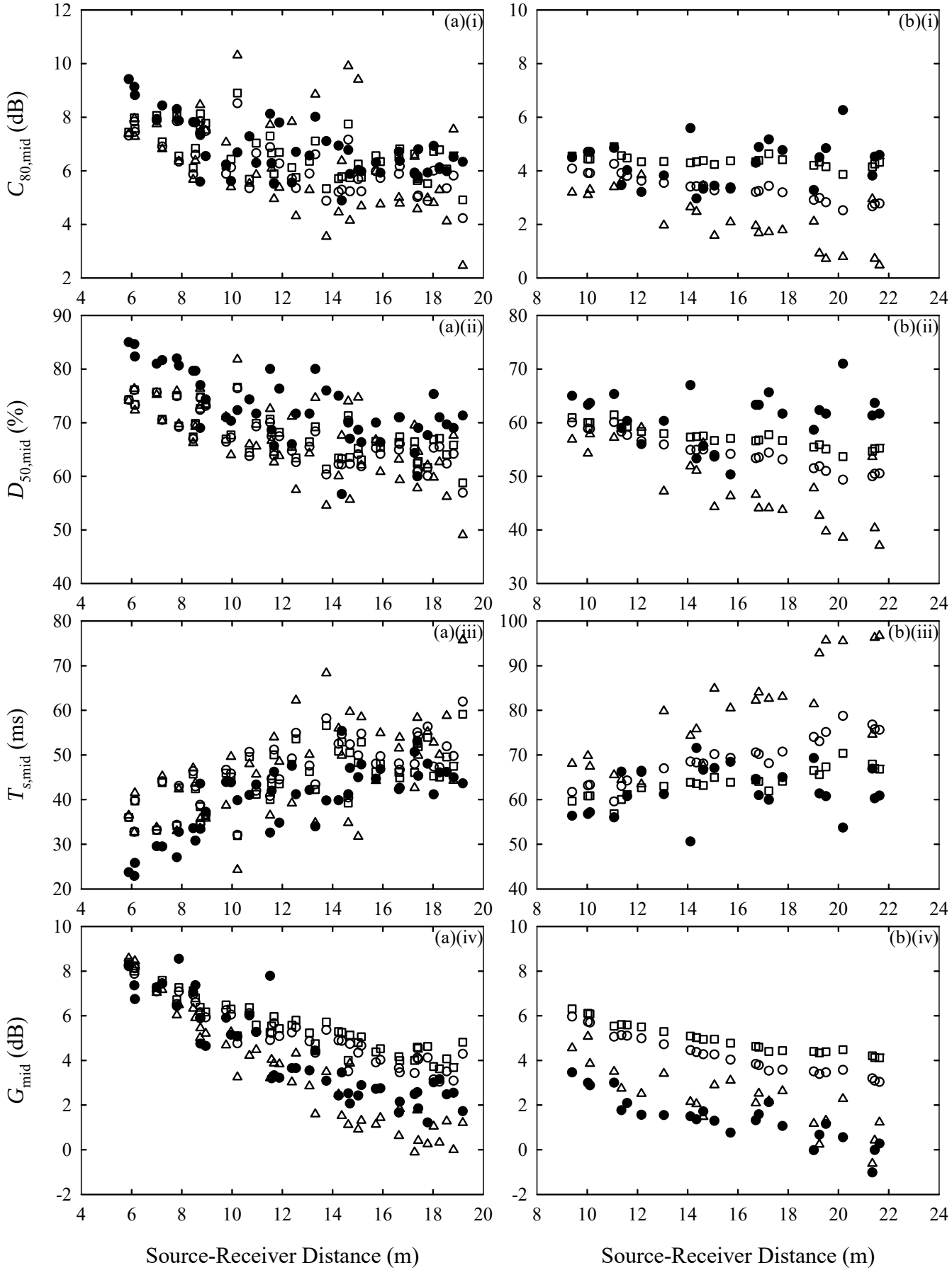

Figure 8 Variations of predicted and measured acoustical parameters with source-receiver distance.
(a) Hall A; (b) Hall B;
(i) $C_{80,mid}$; (ii) $D_{50,mid}$; (iii) $T_{s,mid}$; (iv) G_{mid};
● : measurement; ○ : Barron and Lee [12]; □ : μ-model [17]; △ : Martellotta [16].

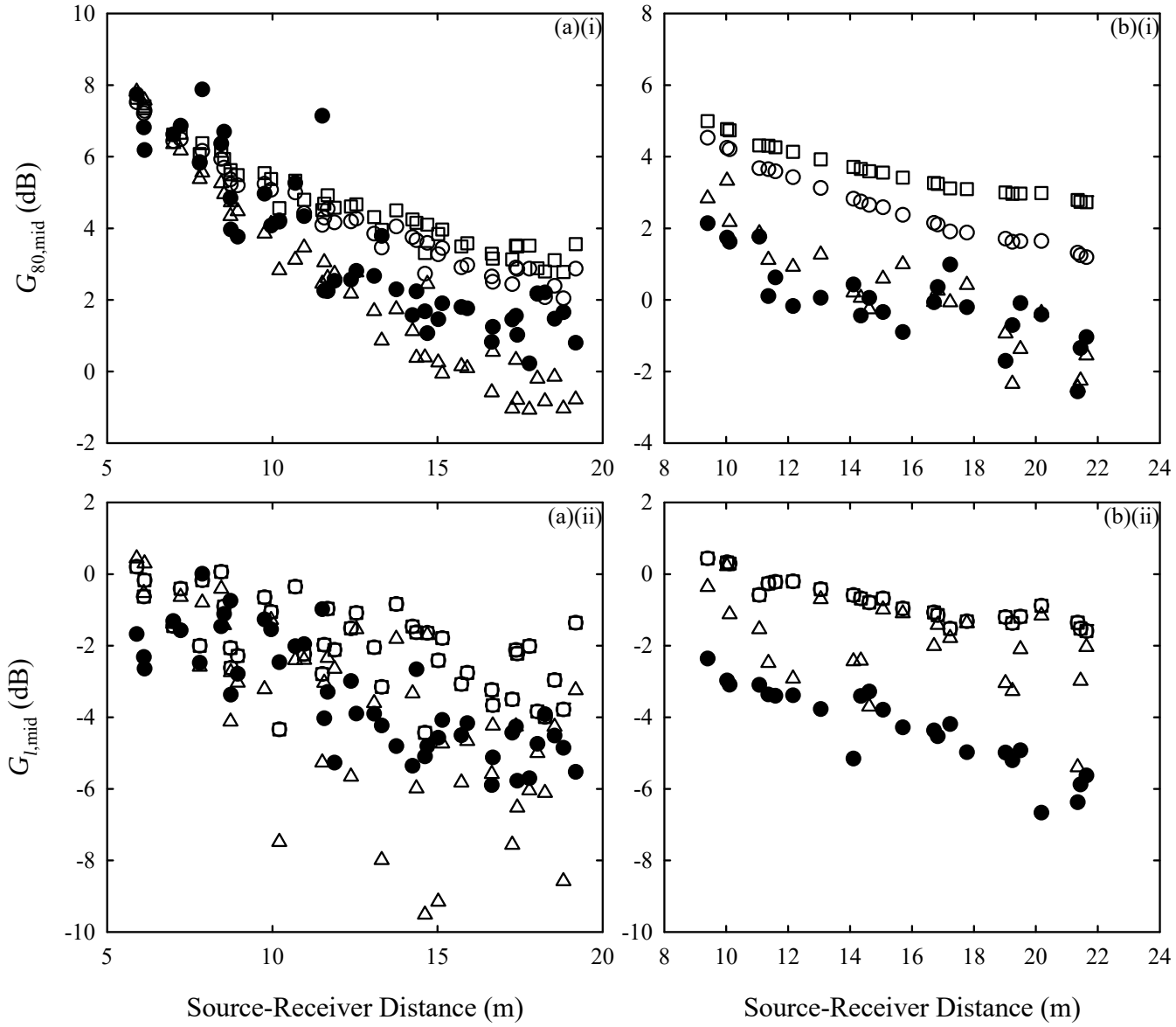

Figure 9 Predictions of early and late sound strengths.
(a) Hall A; (b) Hall B.
(i) $G_{80,mid}$; (ii) $G_{l,mid}$.
● : measurement; ○ : Barron and Lee [12]; □ : μ model [17]; △ : Martellotta [16].

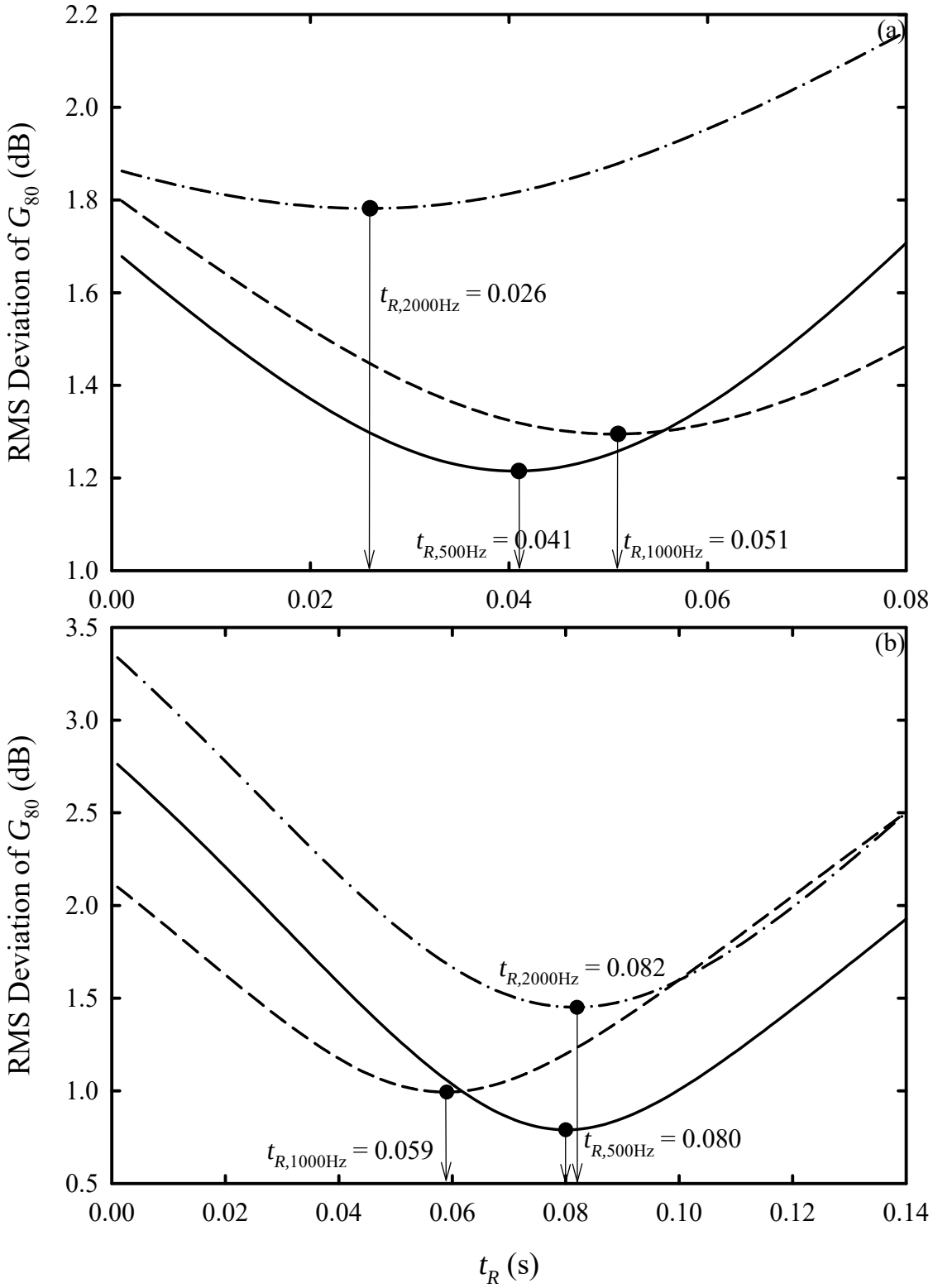

Fig.10 Estimation of the t_R for minimum G_{80} deviation.
(a) Hall A; (b) Hall B.
———— : 500 Hz; – – – – : 1000 Hz; — · — : 2000 Hz.

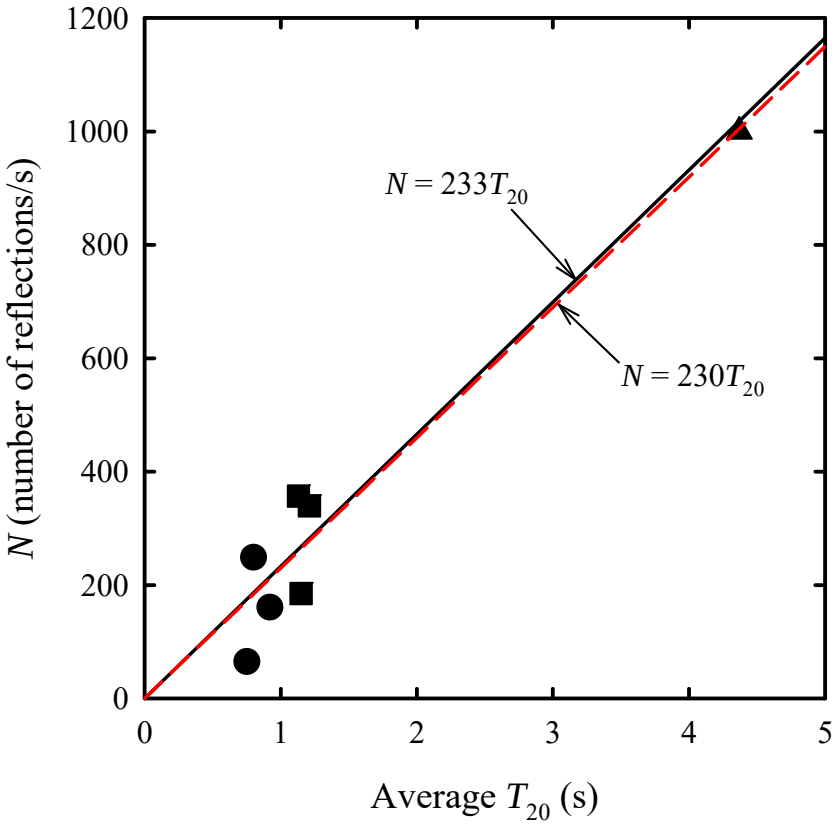

Figure 11 Correlation between N and hall averaged T_{20}.
● : Hall A; ■ : Hall B; ▲: Church data [14];
——— : regression line obtained without the church data;
– – – – : regression line obtained with the church data.

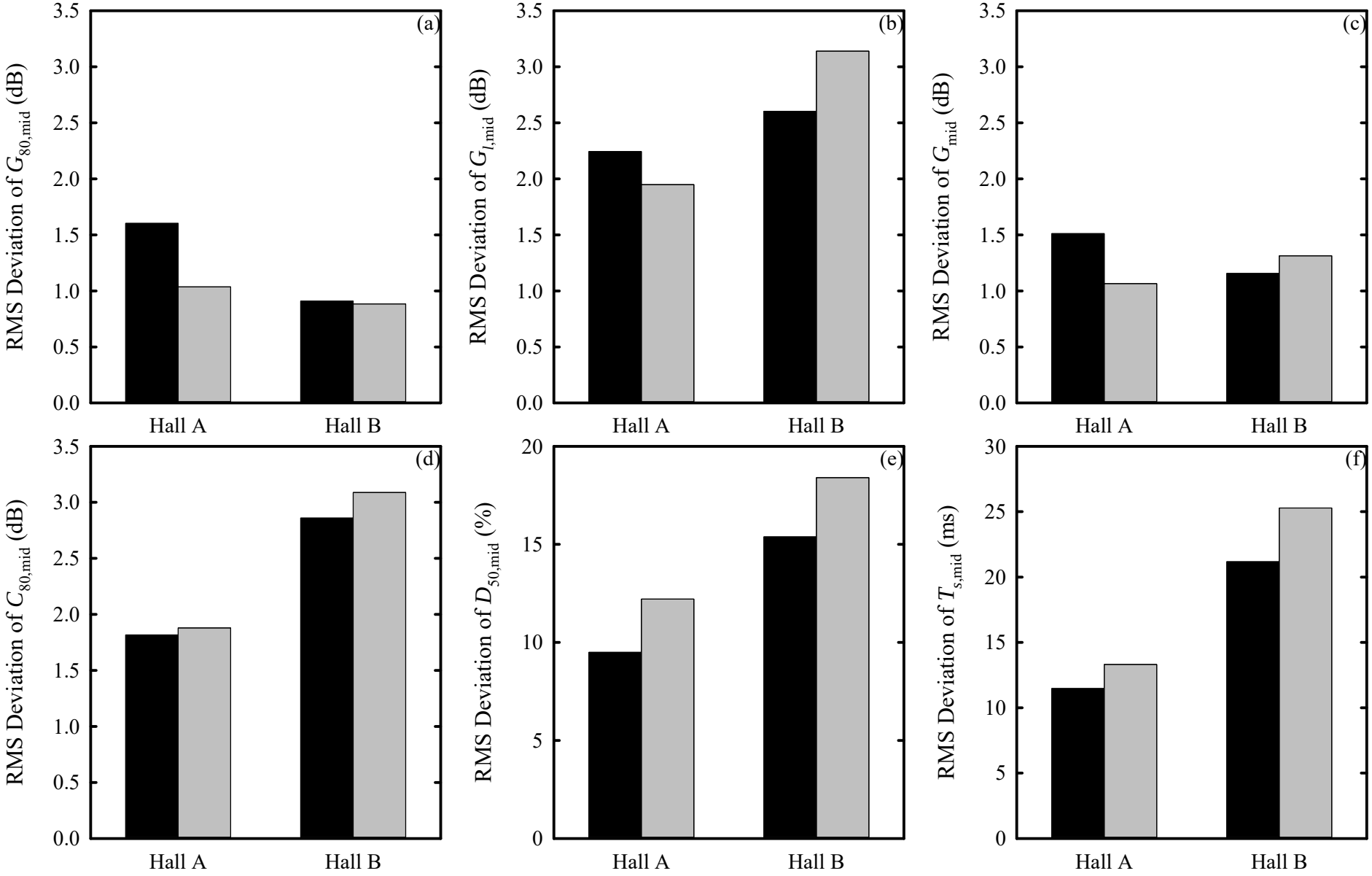

Figure 12 RMS deviations between measured and predicted energy-based acoustical parameters obtained using different t_R estimation methods.
(a) $G_{80,mid}$; (b) $G_{l,mid}$; (c) G_{mid}; (d) $C_{80,mid}$; (e) $D_{50,mid}$; (f) $T_{s,mid}$.
Black bar : point-by-point estimated t_R; grey bar : t_R by Eq. (11).

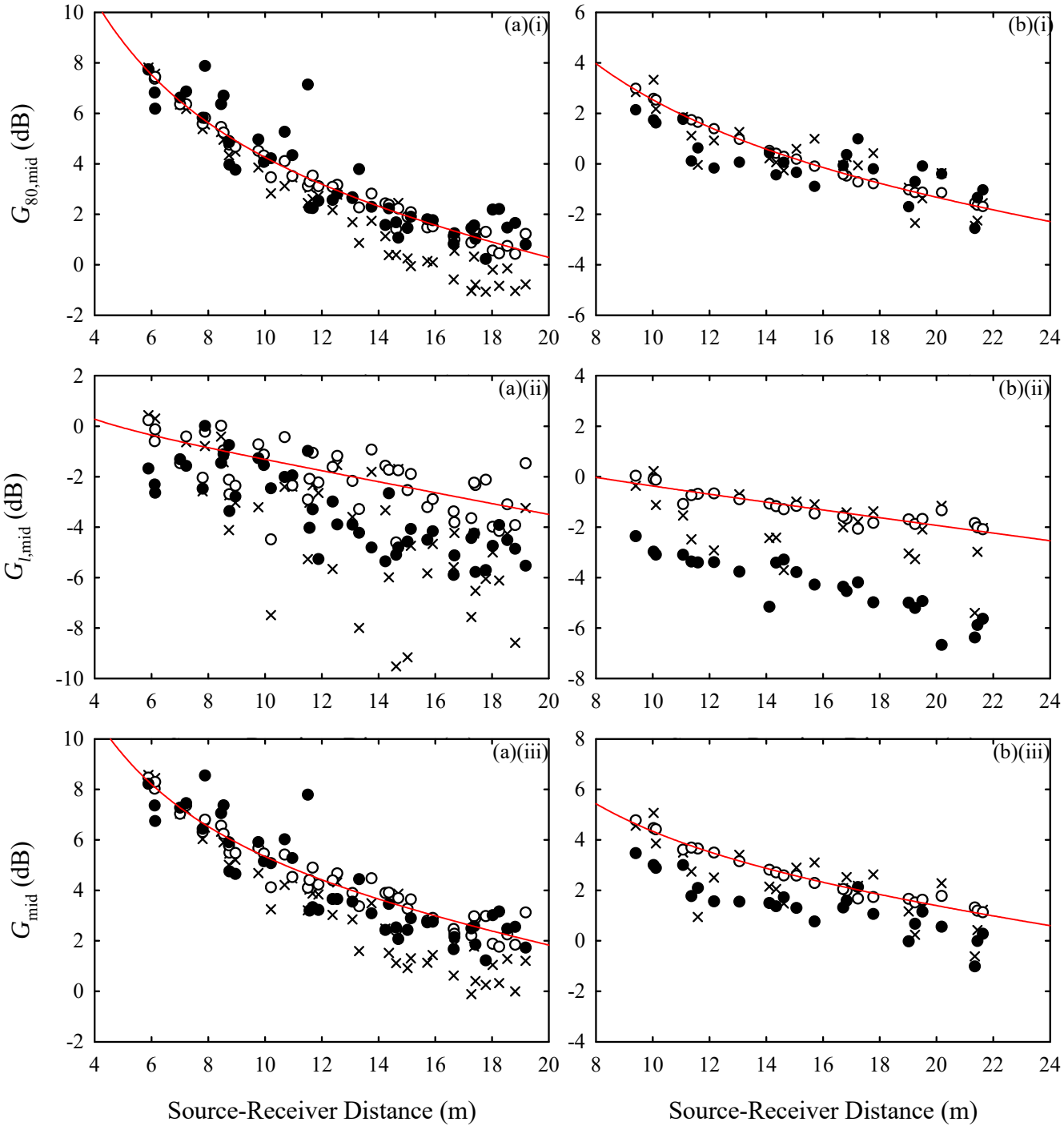

Figure 13 Comparison between predictions of the refined C-M model for sound strengths using the point-by-point estimated t_Rs and the hall averaged t_Rs.
(a) Hall A; (b) Hall B.
(i) $G_{80,mid}$; (ii) $G_{l,mid}$; (iii) G_{mid}.
● : measurements; × : point-by-point estimated t_R ; ○ : hall averaged t_R (Eq. (11)) and local T_{20};
——— : hall averaged t_R (Eq. (11)) and hall averaged T_{20}s.

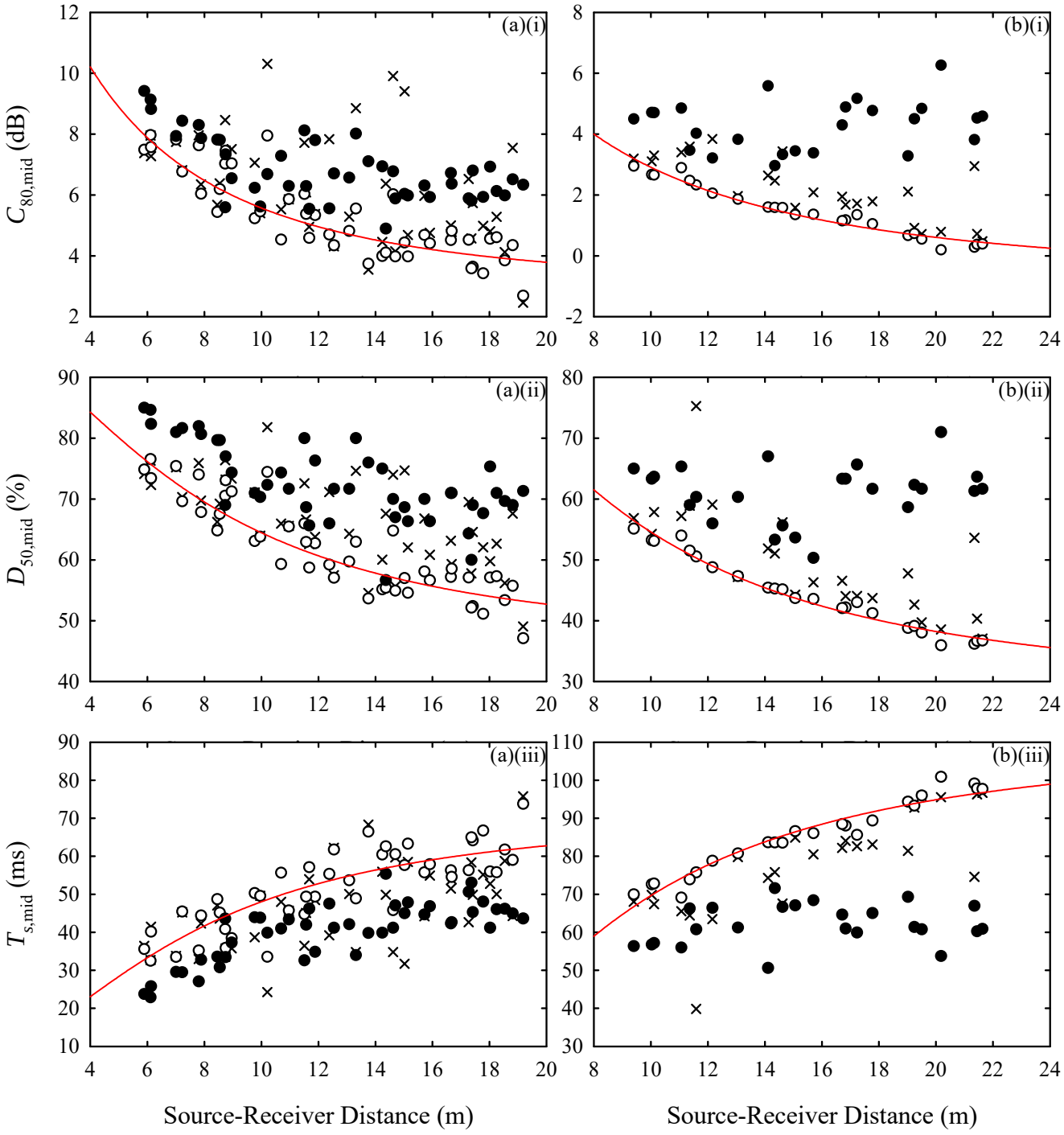

Figure 14 Comparison between predictions of the refined C-M model for clarity, definition and centre time using the point-by-point estimated t_Rs and the hall averaged t_Rs.
(a) Hall A; (b) Hall B.
(i) $C_{80,mid}$; (ii) $D_{50,mid}$; (iii) $T_{s,mid}$.
● : measurements; × : point-by-point estimated t_R ; ○ : hall averaged t_R (Eq. (11)) and local T_{20};
——— : hall averaged t_R (Eq. (11)) and hall averaged T_{20}s.

Table 7
Parameters for t_R estimation.

Parameter	Hall A			Hall B		
	500 Hz	1000 Hz	2000 Hz	500 Hz	1000 Hz	2000 Hz
Average T_{20} (s)	0.92	0.80	0.75	1.21	1.15	1.13
N (reflections/s)	211	185	172	278	264	259
Hall averaged t_R by Eq. (11) (s)	0.047	0.044	0.042	0.072	0.071	0.070

Table 6
Linear regression analysis between predicted and measured sound strengths.

Model	Parameter	Linear Regression Results*	
		Hall A	Hall B
B-L model [12]	G_{mid}	$y = 0.571x + 2.761$, $R^2 = 0.714$	$y = 0.705x + 3.252$, $R^2 = 0.721$
	$G_{80,mid}$	$y = 0.595x + 2.187$, $R^2 = 0.764$	$y = 0.716x + 2.588$, $R^2 = 0.629$
	$G_{l,mid}$	$y = 0.391x – 0.647$, $R^2 = 0.262$	$y = 0.400x + 0.948$, $R^2 = 0.585$
Martellotta [16]	G_{mid}	$y = 1.006x – 0.848$, $R^2 = 0.726$	$y = 1.062x + 0.837$, $R^2 = 0.721$
	$G_{80,mid}$	$y = 1.037x – 1.152$, $R^2 = 0.770$	$y = 1.117x + 0.226$, $R^2 = 0.668$
	$G_{l,mid}$	$y = 0.812x – 1.082$, $R^2 = 0.257$	$y = 0.472x + 0.043$, $R^2 = 0.199$
μ-model [17]	G_{mid}	$y = 0.512x + 3.370$, $R^2 = 0.708$	$y = 0.525x + 4.220$, $R^2 = 0.711$
	$G_{80,mid}$	$y = 0.522x + 2.877$, $R^2 = 0.761$	$y = 0.485x + 3.698$, $R^2 = 0.629$
	$G_{l,mid}$	$y = 0.391x – 0.647$, $R^2 = 0.262$	$y = 0.400x + 0.948$, $R^2 = 0.585$

*y : prediction; x : measurement; R : correlation coefficient.

Table 5
Comparison between predictions and measurements of early and late energies.

Parameter	Prediction Model	Hall A		Hall B	
		$G_{80,\mathrm{mid}}$	$G_{l,\mathrm{mid}}$	$G_{80,\mathrm{mid}}$	$G_{l,\mathrm{mid}}$
Mean Difference	B-L model [12]	0.8 dB	1.4 dB	2.6 dB	3.5 dB
	μ-model [17]	1.3 dB	1.4 dB	3.6 dB	3.5 dB
	Martellotta [16]	-1.0 dB	-0.4 dB	0.2 dB	1.9 dB
RMS Deviation	B-L model [12]	1.4 dB	2.0 dB	2.7 dB	3.6 dB
	μ-model [17]	1.7 dB	2.0 dB	3.7 dB	3.6 dB
	Martellotta [16]	1.6 dB	2.2 dB	0.9 dB	2.6 dB
Slope Difference	B-L model [12]	1.2 dB/10 m	1.3 dB/10 m	-0.3 dB/10 m	1.3 dB/10 m
	μ-model [17]	1.7 dB/10 m	1.3 dB/10 m	0.6 dB/10 m	1.3 dB/10 m
	Martellotta [16]	-1.5 dB/10 m	-1.1 dB/10 m	-1.2 dB/10 m	2.1 dB/10 m

Table 4
Linear regression analysis on correlation between predictions and measurements.

Model	Parameter	Linear Regression Results*	
		Hall A	Hall B
B-L model [12]	$C_{80,mid}$	$y = 0.508x + 2.728$, $R^2 = 0.295$	$y = 0.093x + 3.757$, $R^2 = 0.027$
	$D_{50,mid}$	$y = 0.492x + 31.096$, $R^2 = 0.414$	$y = -0.039x + 56.911$, $R^2 = 0.003$
	$T_{s,mid}$	$y = 0.658x + 19.787$, $R^2 = 0.487$	$y = 0.160x + 59.282$, $R^2 = 0.027$
	G_{mid}	$y = 0.571x + 2.761$, $R^2 = 0.714$	$y = 0.705x + 3.252$, $R^2 = 0.721$
Martellotta [16]	$C_{80,mid}$	$y = 0.484x + 2.936$, $R^2 = 0.087$	$y = -0.471x + 4.223$, $R^2 = 0.148$
	$D_{50,mid}$	$y = 0.433x + 35.243$, $R^2 = 0.153$	$y = -0.247x + 63.789$, $R^2 = 0.029$
	$T_{s,mid}$	$y = 0.639x + 20.65g2$, $R^2 = 0.212$	$y = -0.139x + 88.056$, $R^2 = 0.005$
	G_{mid}	$y = 1.006x – 0.848$, $R^2 = 0.726$	$y = 1.062x + 0.837$, $R^2 = 0.721$
μ-model [17]	$C_{80,mid}$	$y = 0.403x + 3.888$, $R^2 = 0.231$	$y = -0.021x + 4.458$, $R^2 = 0.008$
	$D_{50,mid}$	$y = 0.436x + 36.040$, $R^2 = 0.394$	$y = -0.010x + 57.999$, $R^2 = 0.001$
	$T_{s,mid}$	$y = 0.579x + 21.727$, $R^2 = 0.457$	$y = 0.087x + 58.379$, $R^2 = 0.023$
	G_{mid}	$y = 0.512x + 3.370$, $R^2 = 0.708$	$y = 0.525x + 4.220$, $R^2 = 0.711$

*y : prediction; x : measurement; R : correlation coefficient.

Table 3

Comparison between predictions and measurements of Clarity C_{80}, Definition D_{50}, Centre Time T_s and Sound Strength G.

Parameter	Prediction Model	Hall A				Hall B			
		$C_{80,mid}$	$D_{50,mid}$	$T_{s,mid}$	G_{mid}	$C_{80,mid}$	$D_{50,mid}$	$T_{s,mid}$	G_{mid}
Mean Difference	B-L model [12]	-0.6 dB	-5.8%	6 ms	0.9 dB	-0.9 dB	-6.6%	7 ms	2.8 dB
	μ-model [17]	-0.2 dB	-5.0%	5 ms	1.3 dB	0.1 dB	-3.8%	2 ms	3.6 dB
	Martellotta [16]	-0.6 dB	-6.0%	6 ms	-0.8 dB	-1.8 dB	-11.4%	16 ms	0.8 dB
Mean JND Ratio	B-L model [12]	0.9	1.3	0.7	1.2	1.1	1.4	0.8	2.8
	μ-model [17]	0.8	1.2	0.6	1.5	0.7	1.1	0.4	3.6
	Martellotta [16]	1.5	1.6	0.9	1.2	2.4	2.6	1.8	1.0
RMS Deviation	B-L model [12]	1.1 dB	7.6%	8 ms	1.5 dB	1.4 dB	8.8%	10 ms	2.9 dB
	μ-model [17]	1.0 dB	7.0%	7 ms	1.8 dB	0.9 dB	6.3%	6 ms	3.6 dB
	Martellotta [16]	1.8 dB	9.5%	11 ms	1.5 dB	2.9 dB	15.4%	21 ms	1.2 dB
Slope Difference	B-L model [12]	-0.1 dB/10 m	1.1%/10 m	-2 ms/10 m	1.3 dB/10 m	-1.6 dB/10 m	-9.5%/10 m	10 ms/10 m	0.2 dB/10 m
	μ-model [17]	0.4 dB/10 m	2.4%/10 m	-3 ms/10 m	1.7 dB/10 m	-0.7 dB/10 m	-6.3%/10 m	4 ms/10 m	0.7 dB/10 m
	Martellotta [16]	-0.4 dB/10 m	-0.6%/10 m	1 ms/10 m	-1.2 dB/10 m	-3.3 dB/10 m	-18%/10 m	24 ms/10 m	-0.2 dB/10 m

Table 2
Input parameters of prediction models (t_R is estimated point-by-point).

Model input parameter	Hall A			Hall B		
	500 Hz	1000 Hz	2000 Hz	500 Hz	1000 Hz	2000 Hz
T_{20} (s)	0.92	0.79	0.75	1.19	1.15	1.13
μ (s/m)	0.0296	0.0351	0.0296	0.0197	0.0082	0.0264
α	0.28	0.31	0.32	0.29	0.30	0.29
ζ	0.39	0.16	0.00	0.77	0.64	0.91
Auditorium volume V (m^3)		5350.8			9642.8	
Auditorium surface area S (m^2)		2842.4			3703.1	

Table 1
Basic details of the two halls surveyed.

	Hall A	Hall B
Balcony number	1	1
Seating capacity	1084	1014
Length (m)	26.8	28.0
Width (m)	26.1	30.4
Height (m)	9.7	16.0
Proscenium size (m×m)	14 m (W) × 6.5 m (H)	17.8 m (W) × 10 m (H)
Auditorium volume (m^3)	5350.8	9642.8
Volume of stage house (m^3)	4438.2	16209.9
Volume per seat (m^3)	4.9	9.5
Reverberation time, 1000 Hz (s)	0.79	1.15
Stage wall absorption	No	Yes (perforated plasterboards)
Stage setting	House Curtain + Soft Black Masking (10×Legs + 5×Borders) + Fly Curtains (Cinema Screen + Mid Curtain + Black Drop) + Flat Cyclorama	House Curtain + Soft Black Masking (8×Legs + 4×Borders) + Fly Starry-sky Backdrop + Cyclorama